ELSEVIER

Journal of Organometallic Chemistry 558 (1998) 81–89

Journal of Organometallic Chemistry

Comparison on the selectivity of the first and second attack of selected lithium organyls as nucleophiles on the carbonyls in the bioctahedron complexes $M_2(\mu\text{-}PPh_2)_2(CO)_8$ (M = Mn, Re). Is there a neighbour group effect for the second attack?

H.-J. Haupt *, D. Petters, U. Flörke

Anorganische und Analytische Chemie der Universität-GH Paderborn, Fachbereich 13, Chemie und Chemietechnik, Warburger Straße 100, D-33098, Paderborn, Germany

Received 12 September 1997; received in revised form 26 November 1997

Abstract

In thf solution the bioctahedron complex $Re_2(\mu\text{-}PPh_2)_2(CO)_8$ **1** reacts with one equiv of LiR (R = Ph, Me, *n*Bu, *t*Bu) at temperatures between −90 and −50°C to the acyl monoanion $Li[Re_2(\mu\text{-}PPh_2)_2(CO)_7(ax\text{-}C(R)O)]$ **3** and with a second equiv of LiR^1 (R^1 = Ph, Me, *n*Bu) at 20°C to the diacyl dianions $Li_2[Re_2(\mu\text{-}PPh_2)_2(CO)_6(ax\text{-}C(R)O)(ax\text{-}C(R^1)O)]$ **12** as *trans* or *cis* isomers. Both nearly quantitative reaction steps run selectively: First, both lithium nucleophiles attack exclusively axially coordinated carbonyl ligand. Second, the monoanion with R = Ph forms exclusively the *cis* diacyl dianions (R^1 = *n*Bu, Ph). Through this reaction an anchimeric effect was proved. Third, the monoanions with R = *n*Bu, Me react only to the *trans* diacyl dianions. In general such mono- and dianions have been reacted with O-alkylating agens to the corresponding carbene and dicarbene derivatives (yield 50–70%) to get single crystals for X-ray structure analyses. All products were identified by means of ^1H, ^1P NMR and *v*(CO)IR data. Additionally the molecular structures of the Fischer type carbene complexes $Re_2(\mu\text{-}PPh_2)_2(CO)_7(ax\text{-}C(t\text{Bu})OMe)$ **5b**, *cis*-$Re_2(\mu\text{-}PPh_2)_2(CO)_6(ax\text{-}C(Ph)OEt)_2$ **14** and *trans*-$Re_2(\mu\text{-}PPh_2)_2(CO)_6(ax\text{-}C(n\text{Bu})OMe)(ax\text{-}C(Ph)OMe)$ **15b** are presented. Opposite to **1** affords the homologous dimanganese complex **2** under the same reaction conditions at −50°C with one and two equiv of lithium organyl an unselective nucleophilic addition to axially and equatorially coordinated monoacyl monoanions and diacyl dianions. Our attempts to separate such isomers of the mono- and dianion type as lithium salt led to their decomposition. However, the carbene and dicarbene derivatives $Mn_2(\mu\text{-}PPh_2)_2(CO)_7(ax\text{-}C(Ph)OEt)$ **9ax** and *trans*-$Mn_2(\mu\text{-}PPh_2)_2(CO)_6(ax\text{-}C(n\text{Bu})OEt)_2$ **16** could be crystallized as air-stable, yellow solids. Their molecular structures are presented.

Keywords: Lithium organyls; Nucleophiles; Bioctahedron complexes

1. Introduction

Our earlier studies on the reaction of metal–metal bonded dinuclear group 7 transition metal complexes $M_2(\mu\text{-}PPh_2)(\mu\text{-}H)(CO)_8$ (M = Mn, Re) and nucleophiles LiR (R = aryl, alkyl) allow the generation of mono- and dianions in a selective preparative route achieving cluster expansion reactions with cationic complex fragments on a systematic pathway [1,2]. For dinuclear complexes without a metal–metal bond, e.g. the reaction of $Re_2(\mu\text{-}PPh_2)_2(CO)_8$ **1** and one equiv LiR in thf solution at −90°C, the nucleophilic attack generating the monoanion with an axially coordinated acyl group runs also selectively. At room temperature, however, this anion and one equiv $ClAuPPh_3$ undergo an acylation reaction of gold(I) in which the acyl gold(I) compound is trapped in $Re_2(\mu\text{-}PPh_2)_2(CO)_7(ax\text{-}OC(R)\text{-}AuPPh_3)$ [3].

* Corresponding author. Fax: +49 5251 603423.

0022-328X/98/$19.00
PII S0022-328X(98)00377-5

At the moment our interest in these dinuclear complexes $M_2(\mu\text{-}PPh_2)_2(CO)_8$ (M = Re **1**, Mn **2**) is focused on the title question of this paper. To get an answer the monoanions of **1** and **2** were reacted with different nucleophiles LiR. The nucleophilic attack of the selected lithium organyls which shows no side-reaction was analyzed by ^{31}P NMR and ν(CO) IR data. Although we could not grow single crystals from the lithium salts, their conversion to the Fischer type carbene derivatives [4] provided suitable samples for X-ray structure determinations which ascertain the position of the acyl groups. This study is partly parallel to the earlier synthesis of acyl monoanions as intermediates from group 7 transition metal (M) decacarbonyls and lithium organyls [5]. Further elegant synthetic routes are known [6–11]. With regard to the title question it must be stated that until now the reaction behaviour of the acyl monoanions is not investigated. Additionally, acyl and diacyl anions including the corresponding carbene and dicarbene derivatives are hitherto unknown for the twofold diorganophosphido bridged complexes **1** and **2**. Perhaps this kind of complex offers a future preparative route for regio- and stereoselective combination with an appropriate compound to generate allene type systems and, further, may be of interest for metathesis reactions [12,13]

2. Results and discussion

2.1. Preparations with $M_2(\mu\text{-}PPh_2)_2(CO)_8$ (M = Re **1**, Mn **2**)

As described in the previous paper [3], in thf solution of **1** the nucleophilic attack of the reagent LiR at −90°C affords within 15 min the subsequently named acyl monoanions as lithium salts $Li[Re_2(\mu\text{-}PPh_2)_2(CO)_7(ax\text{-}C(R)O)]$ (R = Ph **3a**, Me **3b**, *n*Bu **3c**, *t*Bu **3d**). (Scheme 1, (i)). According to ^{31}P NMR data of the reaction solutions, the axial attack of R^- runs selectively in all considered reaction systems at least in the temperature range from −90 to −50°C, but quantitatively only for **3a**–**c**. The yield of **3d** is distinctly lower because the stronger nucleophile *t*BuLi forms a known byproduct via a thf alkylation reaction [14]. The lithium salts **3a**–**d** react to the crystalline carbene derivatives $Re_2(\mu\text{-}PPh_2)_2(CO)_7(ax\text{-}C(R)OEt)$ (R = Ph **4a**, Me **4b**) and $Re_2(\mu\text{-}PPh_2)_2(CO)_7(ax\text{-}C(R)OMe)$ (R = *n*Bu, **5a**, *t*Bu **5b**) on the mostly used synthetic route with the O-alkylating reagents like Me_3OBF_4 and Et_3OBF_4 in a convenient solvent at room temperature (Scheme 1, (iii)). The use of the weaker O-alkylation reagent CF_3SO_3Et needs a more time-consuming reaction process. As a further disadvantage, this leads to a known competive ring opening process of thf which is partly coordinated at the lithium cations in **3a**–**d**. The reaction gives a byproduct with $R = O(CH_2)_4OEt$. The adherence of the axial substitution pattern in the bioctahedron is based on the measured ^{31}P NMR data. In addition the ^1H NMR data show that only the *Z* isomer of the carbene group is formed. The spectroscopic data indicate no *E*/*Z* isomerization. These structural features are confirmed from the molecular structure of solid **5b** (Fig. 1).

Opposite to **1**, in thf solution the dimanganese complex **2** and one equiv LiR afford at −50°C instead of −90°C the isomeric products $Li[Mn_2(\mu\text{-}PPh_2)_2(CO)_7)(ax/eq\text{-}C(R)O)]$ (R = Ph **6ax**/**eq**, Me **7ax**/**eq**, *n*Bu **8ax**/**eq**). The lesser solubility of **2** against that of **1** demands the higher reaction temperature of −50°C. Attempts to precipitate the lithium salts triggers decomposition. Only the subsequent conversion of each acyl isomer mixture to the monocarbenes generates the isolable derivatives $Mn_2(\mu\text{-}PPh_2)_2(CO)_7(ax/eq\text{-}C(R)OEt)$ (R = Ph, **9ax**/**eq**, Me **10ax**/**eq**, *n*Bu **11ax**/**eq**) Fig. 2. For correct assignment a comparison of the ^{31}P and ^1H NMR data with those of **4a**,**b** was helpful. Further support results from the spectroscopic data of the ax-isomer **9ax** which crystallizes from a solution of **9ax**/**eq** whereas the other isomer decomposes. The given assignments are unambiguous (see Section 3, Experimental details) in spite of the presence of the quadruple manganese nuclei in the ^1H and ^{31}P NMR spectra. The missing signal of the $^2J_{PP}$ coupling frequency in each of the eq-isomers via low-temperature measurements down to 233 K in $CDCl_3$ was not detectable. The ^1H NMR data of the ethoxy group agree with the ratio of the ax/eq isomers: 1/1.4 in **9ax**/**eq**, 7.5/1 in **10ax**/**eq** and 4/1 in **11ax**/**eq**.

To examine our idea of a selective nucleophilic attack for a second equiv of LiR^1, it was evident from the described preparative results that these experiments should mainly be focused on the dirhenium complexes **3a**–**d**. Already the first experiments showed that in thf solution each of the denoted monoanions needs at least room temperature to be attacked by the same nucleophile. A systematic alteration of the residues R and R^1 in the nucleophiles for the dianion formation leads to the following results (Scheme 1, (ii)): First, the nucleophile LiR^1 affords exclusively the diaxial attachment of both acyl groups in the dianions. Second, the monoanion **3a** (R = Ph) forms the *cis* dianion in the salts $Li_2[cis\text{-}Re_2(\mu\text{-}PPh_2)_2\text{-}(CO)_6(ax\text{-}C(Ph)O(ax\text{-}C(R^1)O)]$ (R^1 = Ph **12a**, *n*Bu **12b**) as unique reaction product. Third, the monoanions **3b**–**d** deliver selectively the *trans* dianion in the salts $Li_2[trans\text{-}Re_2(\mu\text{-}PPh_2)_2(CO)_6(ax\text{-}C(R)O)(ax\text{-}C(R^1)O]$ (R = *n*Bu, R^1 = *n*Bu **13a**, Ph **13b**; R = Me, R^1 = Me **13c**, Ph **13d**). Each of the geometrical isomers is separable as an air-stable yellow salt in nearly quantitative amounts. The observed number of the υ(CO) IR absorption bands for the *cis* dianion is five and three for the *trans* dianion

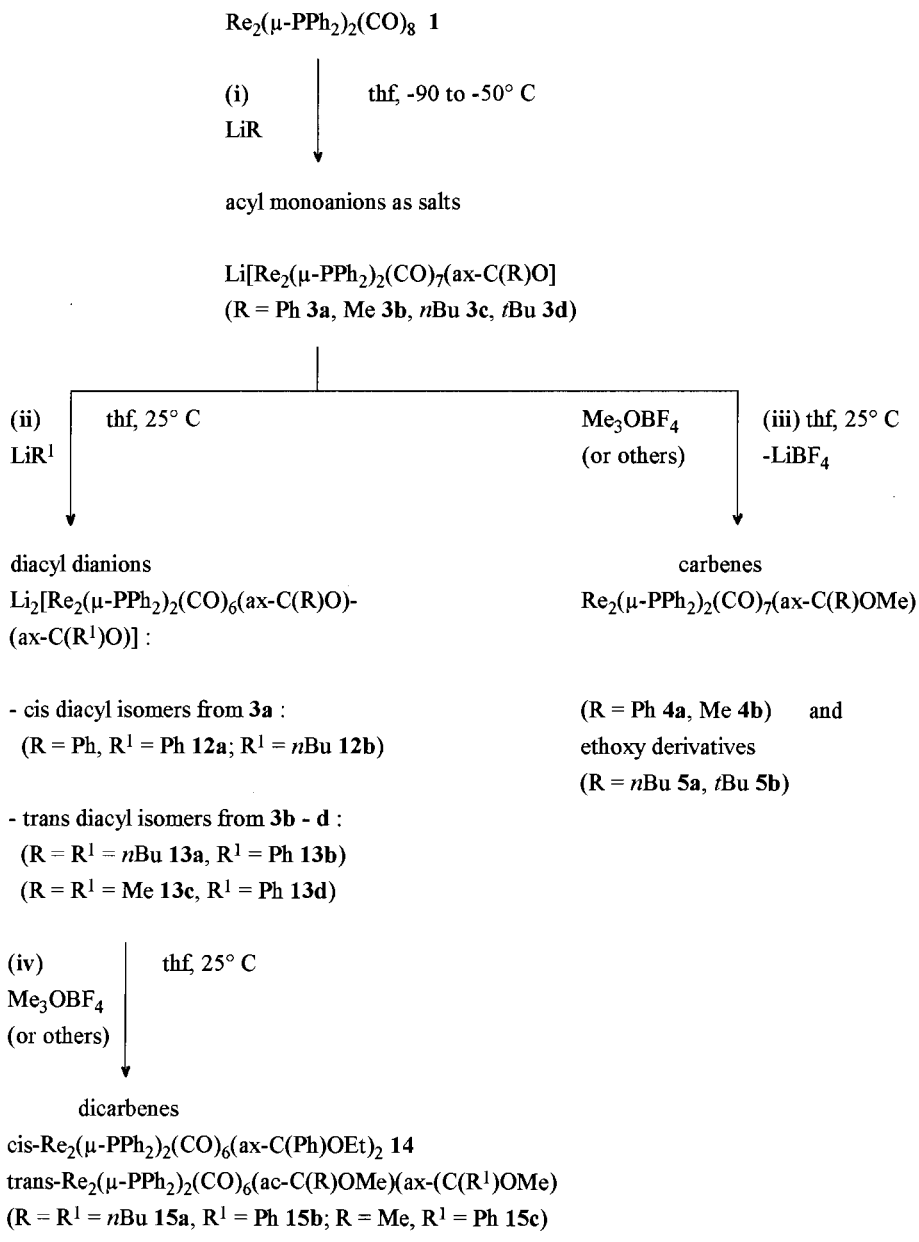

Scheme 1.

and correspond with group theoretical considerations. The υ(CO) IR mode of the acyl group appears at 1540 cm^{-1} in **13a**. Further spectroscopic characterization was done by means of ^{31}P and ^{1}H NMR measurements as given in Experimental details.

The subsequent derivatization of the dianions **12a**, **13a**, **13b**, **13c** with two equiv of the corresponding O-alkylation agens in thf solution at room temperature gives the dicarbenes as yellow and air-stable solids in yields of 50–70%: *cis*-$Re_2(\mu\text{-}PPh_2)_2(CO)_6$(ax-C(Ph)--$OEt)_2$ **14**, *trans*-$Re_2(\mu\text{-}PPh_2)_2(CO)_6$(ax-C(R)OMe)(ax-$C(R^1)OMe$) ($R = R^1 = n$Bu **15a**, R^1 = Ph **15b**; R = Me, R^1 = Ph **15c**). These dicarbenes have been identified by ^{1}H and ^{31}P NMR data and X-ray structure analyses (Figs. 3–5).

The mentioned *cis* dianions **12a–b** are formed in a kinetically controlled reaction. The contribution of at least one phenyl group at the μ-P atoms in the neighborhood of the axially attached carbonyl ligand in the phenylacyl monoanion **3a** was investigated by reaction of complex $Re_2(\mu\text{-}PEt_2)_2(CO)_8$ instead of the phenyl complex **1** with the nucleophiles LiR (R = Ph, *n*Bu) under the same conditions. These in situ experiments were accompanied by ^{31}P NMR measurements and confirmed that, independent on LiR, a molar reaction ratio of 1:1 results in the salts Li[$Re_2(\mu\text{-}PEt_2)(CO)_7$(ax-C(R)O)] ($\delta$ ^{31}P (THF): R = Ph, −180.5 (s, 2P, μ-P); R = Bu, −179.8 (s, 2P, μ-P)) and a reaction ratio of 1:2 always results in the salts *trans*-$Li_2[Re_2(\mu\text{-}PEt_2)(CO)_6(C(Bu)O)(C(Ph)O)]$ (δ ^{31}P (THF) −181.0 (s,

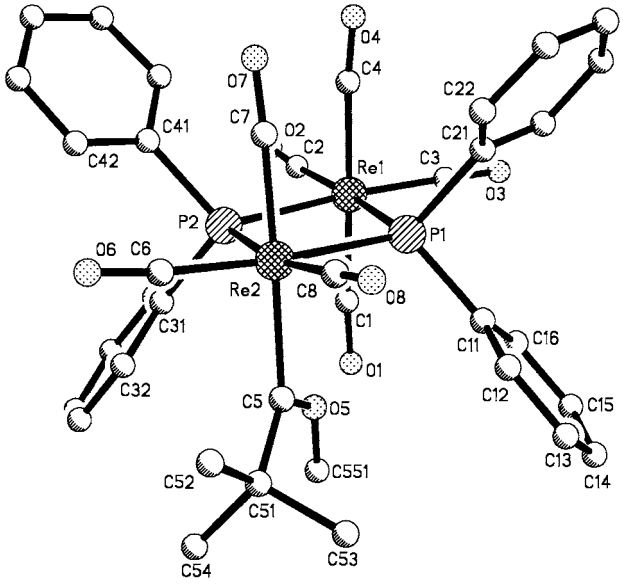

Fig. 1. Molecular structure of **5b** with hydrogen atoms omitted.

2P, μ-P). This shows undoubtedly that in **1** a phenyl ligand of the μ-P atom is involved in a transition state directing the stereoselectivity on the formation of the *cis* dianions **12a**–**b**.

The analogous experiments with the dimanganese monoanions and LiR^1 in the thf solution allow no separation of dianions. To obtain an isolable dicarbene derivative, **2** and two equiv *n*BuLi in thf solution at room temperature reacted in the first step to a mixture of the ax/eq-isomeric dianions. Then these intermediates and two equiv of Et_3OBF_4 react to a mixture of dicarbenes in solution from which only *trans*-$Mn_2(\mu$-

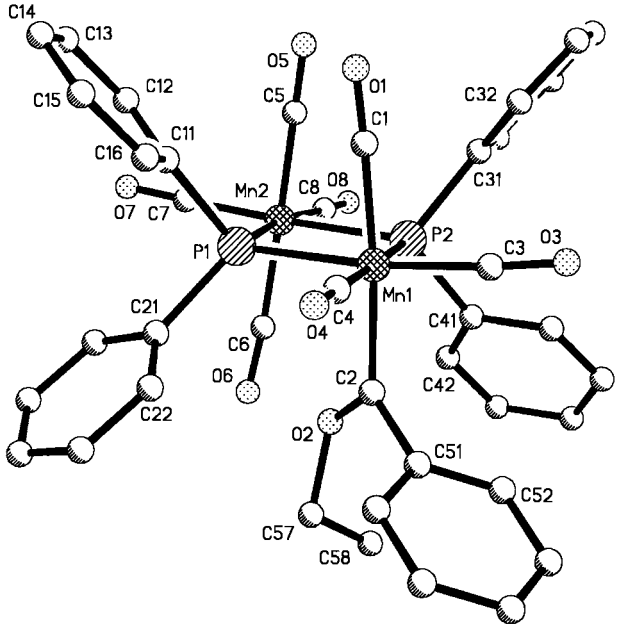

Fig. 2. Molecular structure of **9ax** with hydrogen atoms omitted.

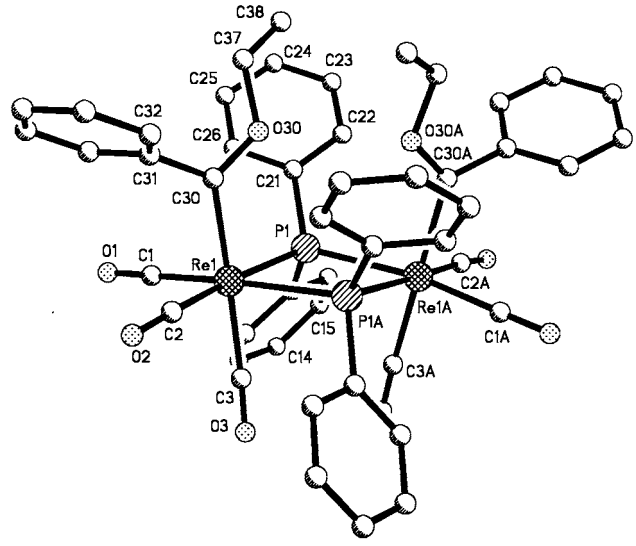

Fig. 3. Molecular structure of **14** (conformer A) with hydrogen atoms omitted.

$PPh_2)_2(CO)_6$(ax-C(*n*Bu)OEt)$_2$ **16** (Fig. 6) precipitates. The unidentified other dimanganese product decomposes.

2.2. Molecular structures of carbenes and dicarbenes

2.2.1. Carbenes

$Re_2(\mu$-$PPh_2)_2(CO)_7$(ax-C(*t*Bu)OMe) **5b**. The molecule (Fig. 1) represents an edge-bridged bioctahedron complex with two diorganophosphido bridges as edges, seven carbonyl ligands and the axially coordinated carbene group. These eight terminal ligands show almost ecliptic arrangement viewed along the Re···Re vector with torsion angles ranging from 2.3 to 11.6°. The central molecular fragment is a four-membered nearly planar Re_2P_2 ring with a dihedral angle ReP_2/P_2Re of 4.1. The nonbonding Re···Re distance of 3.971(2) Å is somewhat enlarged opposed to that of 3.928(1) Å in $Re_2(\mu$-$PPh_2)_2(CO)_8$ [15] due to the substitution of one axial carbonyl group vs the carbene ligand. The resulting Re-carbene C5 bond distance of 2.18(3) Å is at the

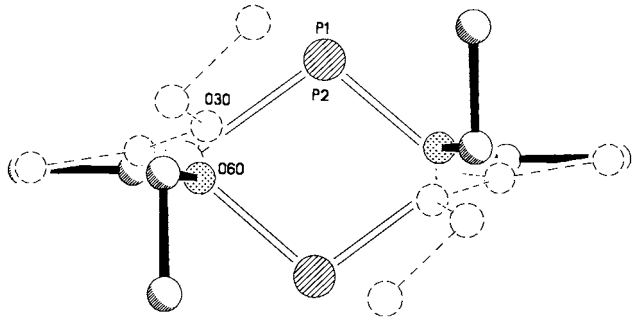

Fig. 4. Superposition of conformeres A (dashed) and B (solid) of 14. Phenyl groups and hydrogen atoms omitted.

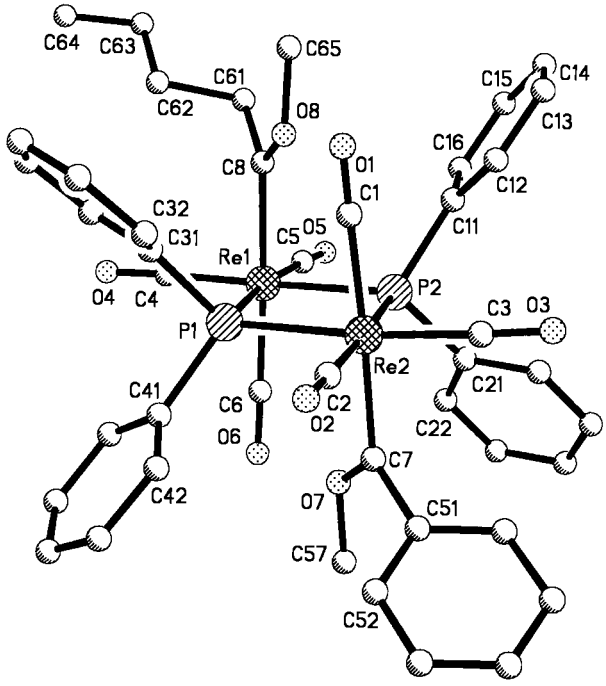

Fig. 5. Molecular structure of **15b** with hydrogen atoms omitted.

upper limit of reported Re-carbene C distances and may be compared to that of 2.08(1) Å in $Re_2(CO)_9$(ax-C(*n*Bu)OEt) [9], of 2.09(1) Å in $MnRe(CO)_9$(ax-C(Me)OMe) [7]a, or of 2.125(9) Å in $[(CO)_5ReC(C_3H_6O)]^+$ [16]. The vector of the carbene C5–O bond is oriented parallel to the Re···Re direction with a torsion angle Re1–Re2–C5–O5 of 6.2° and the orientation of the carbene ligand along the Re=C bond shows *Z* configuration. Similar geometrical features are also valid for the molecular structures of the related monocarbenes $Re_2(\mu\text{-}PPh_2)_2(CO)_7$(ax-C(*n*Bu)OEt), $Re_2(\mu\text{-}PPh_2)_2(CO)_7$(ax-C(*n*Prop)OEt) (U. Flörke, H.-J. Haupt, D. Petters, unpublished results) and the dimanganese derivative $Mn_2(\mu\text{-}PPh_2)_2(CO)_7$(ax-C(Ph)OEt) **9ax**, shown in Fig. 2. For this latter complex the related torsion angle Mn2–Mn1–C2–O2 of the carbene ligand is 10.6° and the Mn_2P_2 ring shows only slight deviation from planarity with a dihedral angle MnP_2/P_2Mn of 1.6°. The Mn–C2 bond length of 1.954(7) Å is also in the upper range of reported Mn-carbene distances [17–21].

2.2.2. Dicarbenes

cis-$Re_2(\mu\text{-}PPh_2)_2(CO)_6$(ax-C(Ph)OEt)$_2$ **14**. There are two independent molecules (A and B) per asymmetric unit, each lying on a crystallographic twofold axis which runs vertically through the midpoints of the Re_2P_2 planes. Both molecules show as common structural feature the central Re_2P_2 ring with each Re atom connected to three terminal carbonyl ligands and to one axially coordinated carbene group with *Z* configuration (Fig. 3). As for the monocarbene structures these ligands show ecliptic arrangement, too. The carbene torsion angles Re–Re–C–O for molecules A and B are different with 15.0° for A and only 0.5° for B, respectively. Furthermore, the positions of the ethoxy groups display two different possibilities for avoiding short non-bonding intramolecular contacts which otherwise would arise from the sterically unfavourable *cis*-arrangement of the carbene ligands. In molecule A the C–C vector of the ethyl group is almost parallel to the Re–P bond with torsion angle P–Re–C37–C38 of 4.1 and Re–Re–C37–C38 of 41.8. In molecule B the Re···Re and the C–C vectors are perpendicular with torsion angle P–Re–C67–C68 of 123.5° and Re–Re–C67–C68 of 85.6°. Fig. 4 shows the different OEt-group arrangements for conformeres A and B. Additionally, the Re_2P_2 ring is no longer planar but folded with an dihedral angle ReP_2/P_2Re of 10.4° (average value for A and B). This also allows better stacking of the carbene ligands, whereas the carbonyl groups **3** and **3a** on the opposite side of the Re_2P_2 ring are not so sterically demanding. Similar ring folding due to ligand substitution has been observed earlier [22]. *trans*-$Re_2(\mu\text{-}PPh_2)_2(CO)_6$(ax-C(*n*Bu)OMe)(ax-C(Ph)OMe) **15b**. In contrast to **14** this type of geometrical isomer (Fig. 5) shows no steric crowding due to the anti-position of the two different carbene ligands. As consequence the Re_2P_2 ring is planar with a dihedral angle ReP_2/P_2Re of only 0.9°. Again the carbene groups show *Z* configuration and the torsion angles which indicate their orientation parallel to the Re···Re vector are Re1–Re2–C7–O7 7.7° and Re2–Re1–C8–O8 4.9°, respectively. Further bond lengths and angles show no unexpected features (Table 1) and compare well with the above discussed geometries as well as with those of the related compounds *trans*-$Re_2(\mu\text{-}PPh_2)_2(CO)_6$(ax-C(*n*Bu)$OC_4H_8$Et)$_2$ (U. Flörke, H.-J. Haupt, D. Petters, unpublished results). and *trans*-$Mn_2(\mu\text{-}PPh_2)_2(CO)_6$(ax-C(*n*Bu)OEt)$_2$ **16** (Fig. 6). Complex **16** shows similar molecular geometry as **15b** with *trans* position of the carbene ligands. The centre of the molecule lies on a crystallographic inversion centre which implies a planar Mn_2P_2 ring. The carbene ligand has again *Z* configuration, with the C–O bond parallel to the Mn···Mn vector indicated by the torsion angle Mn–Mn–C4–O4 of 2.9°. The carbene OEt group shows the same perpendicular arrangement relative to the Mn···Mn direction known from the B conformere of molecule **14** with torsion angle Mn–Mn–C9–C10 of 85.5°.

2.3. Conclusion

The title question can be enlightened from the experimental results which show that an anchimeric effect could be proved, for example, by the quantitative conversion of the phenylacyl monoanion **3a** with LiR^1

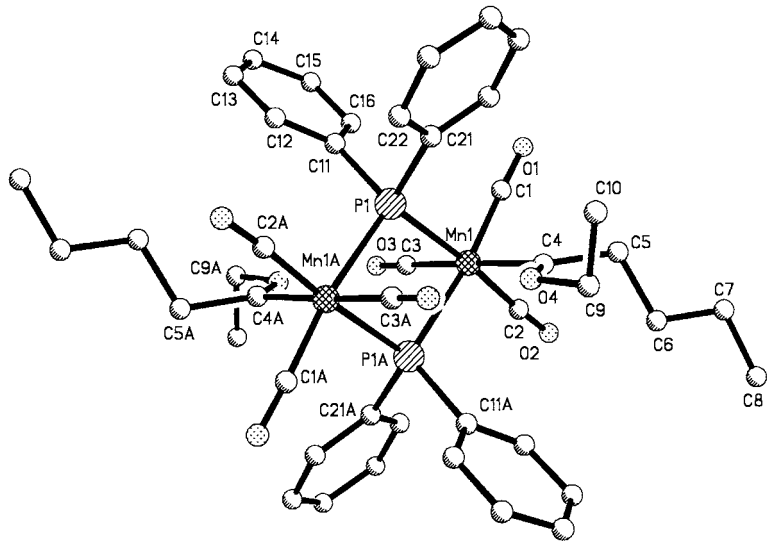

Fig. 6. Molecular structure of **16** with hydrogen atoms omitted.

(R^1 = alkyl, aryl) to the thermodynamically not favoured *cis* isomers **12a** and **12b**. At present it can be stated that one of the factors influencing the formation of such *cis* dianions as Li salts is a phenyl group attached to the μ-P atom. Furthermore the dependency of a Li^+ coordination at the phenacyl group can be excluded. The complete removal of Li^+ by an appropriate chelate (12-crown-4-ether) maintains the original selectivity of the second LiR attack. Additional computational studies show that free rotation of the phenacyl ligand around the $Re-C_{acyl}$ bond in monoanion **2a** is hindered from the μ-PPh_2 groups. A second attack at the CO ligand *cis* to the phenacyl residue including the mentioned contribution of a μ-P phenyl ligand may therefore be supported by either stabilization of a transition state with intermediate crowding of phenyl groups or by an electronic effect of the aryl group or even by both factors. Further elucidation is expected from preparation of monoanions with other ligands than phenyl attached to the acyl group.

3. Experimental details

All reactions were carried out in solvents free of oxygen which were dried according to literature methods, distilled and stored under argon atmosphere. The reaction products were characterized by υ(CO) FTIR spectroscopy (Nicolet P510), ^1H and ^{31}P NMR spectroscopy (Bruker AMX 300).

3.1. Chemicals

$Re_2(CO)_{10}$, (Acros), NPPCl and $HPPh_2$ (Strem), 1.6 M PhLi, 1.6 M MeLi, 1.6 M BuLi, 1.5 M *t*BuLi, 1 M Et_3OBF_4, Me_3OBF_4 and CF_3SO_3Et (Fluka) were purchased. The compounds $M_2(\mu\text{-}PPh_2)_2(CO)_8$ (M = Mn [23], M = Re [24]) and $Mn_2(CO)_{10}$ [25] were prepared according to literature methods.

3.2. Preparation

3.2.1. Carbenes

$Re_2(\mu\text{-}PPh_2)_2(CO)_7$(ax-C(R)OEt) (R = Ph **4a**, Me **4b**) and $Re_2(\mu\text{-}PPh_2)_2(CO)_7$(ax-C(R)OMe) (R = *n*Bu **5a**, *t*Bu **5b**). According to the preparative procedure in [3], each salt $Li[Re_2(\mu\text{-}PPh_2)_2(CO)_7$(ax-C(R)O)] (R = Ph **3a**, Me **3b**, *n*Bu **3c**, *t*Bu **3d**) (0.155 mmol) was dissolved in 10 ml $CHCl_3$ and reacted at room temperature with the equimolar amount of Et_3OBF_4 or Me_3OBF_4. After stirring for 30 min, the products were separated by column chromatography (neutral Al_2O_3) with CH_2Cl_2/*n*-hexane 1/1 as eluant. There was only one yellow main fraction which contained the carbenes. The solvent was removed in vacuo and yellow crystals (yield) remained: 105 mg (65%) **4a**, 63 mg (40%) **4b**, 100 mg (62%) **5a**, and 90 mg (56%) **5b**.

$Mn_2(\mu\text{-}PPh_2)_2(CO)_7$(ax/eq-C(R)OEt) (R = Ph **9ax**/**eq**, Me **10ax**/**eq**, *n*Bu **11ax**/**eq**). One equiv of LiR in cyclohexane/ether solution was added at −50°C to 10 ml thf solution $Mn_2(\mu\text{-}PPh_2)_2(CO)_8$ **2** (100.7 mg; 0.155 mmol). On warming up to room temperature, the colour of the solution changed from yellow via green to orange. The solvent was removed in vacuo, and the residue $Li[Mn_2(\mu\text{-}PPh_2)_2(CO)_7$(ax/eq-C(R)O)] (ax/eq isomer mixture: R = Ph **6ax**/**eq**; Me **7ax**/**eq**; *n*Bu **8ax**/**eq**) was dissolved in CH_2Cl_2 with red colour. The addition of one equiv Et_3OBF_4 gave within 15 min the carbene. The products were separated chromatographically by use of PLC plates (silicagel 60 F_{254}, Merck). The ratio of the isomers was derived from the ^1H NMR data of the alkoxy group, and the following red crys-

talline products remained after evaporation of the solvents in vacuo (amount): **9ax**/**eq** separated with the eluant CH_2Cl_2/*n*-hexane 1/2, isomer ratio 1/1.4, 54 mg (46%); **10ax**/**eq**, 1/2, 45 mg (39%); **11ax**/**eq**, CH_2Cl_2/*n*-hexane 1/1 as eluant, 1/1, 70 mg (70%). It was possible to separate small amounts of the ax-isomer by fractionated crystallization.

Table 1
Selected bond distances [Å] and angles [°]

5b			
Re1–P1	2.533(6)	P1–Re1–P2	76.5(2)
Re1–P2	2.524(7)	P1–Re2–P2	76.4(2)
Re2–P1	2.523(7)	Re1–P1–Re2	103.5(2)
Re2–P2	2.538(6)	Re1–P2–Re2	103.3(2)
Re2–C5	2.18(3)	Re2–C5–O5	112(2)
C5–O5	1.27(3)		
C5–C51	1.58(4)		
Re1···Re2	3.971(1)		
9ax			
Mn1–P1	2.402(2)	P1–Mn1–P2	77.75(6)
Mn1–P2	2.379(2)	P1–Mn2–P2	77.49(6)
Mn2–P1	2.396(2)	Mn1–P1–Mn2	102.07(7)
Mn2–P2	2.399(2)	Mn1–P2–Mn2	102.65(7)
Mn1–C2	1.954(7)	Mn1–C2–O2	121.3(4)
C2–O2	1.311(7)		
C2–C51	1.509(8)		
Mn1···Mn1	3.731(1)		
14			
Molecule A			
Re1–P1	2.527(2)	P1–Re1–P1a	75.87(7)
Re1–P1a	2.540(2)	Re1–P1–Re1a	103.65(7)
Re1–C30	2.131(10)	Re1–C30–O30	121.0(7)
C30–O30	1.312(11)		
Re1···Re1a	3.983(1)		
Molecule B			
Re2–P2	2.539(2)	P2–Re2–P2a	75.53(7)
Re2–P2a	2.525(2)	Re2–P2–Re2a	103.73(7)
Re2–C60	2.106(10)	Re2–C60–O60	120.9(6)
C60–O60	1.344(10)		
Re2···Re2a	3.983(1)		
15b			
Re1–P1	2.531(5)	P1–Re1–P2	75.73(14)
Re1–P2	2.538(4)	P1–Re2–P2	75.95(14)
Re2–P1	2.537(4)	Re1–P1–Re2	104.0(2)
Re2–P2	2.520(5)	Re1–P2–Re2	104.3(2)
Re1–C8	2.12(2)	Re1–C8–O8	120.3(12)
C8–O8	1.30(2)	Re2–C7–O7	121.9(12)
Re2–C7	2.08(2)		
C7–O7	1.31(2)		
C7–C57	1.45(2)		
C8–C65	1.46(2)		
Re1···Re2	3.994(1)		
16			
Mn1–P1	2.404(1)	P1–Mn1–P1a	76.16(4)
Mn1–P1a	2.414(1)	Mn1–P1–Mn1a	103.84(4)
Mn1–C4	1.977(4)	Mn1–C4–O4	119.9(3)
C4–O4	1.310(4)		
Mn1···Mn1a	3.793(1)		

3.2.2. Dicarbenes

$Li_2[cis\text{-}Re_2(\mu\text{-}PPh_2)_2(CO)_6(ax\text{-}C(R)O)(ax\text{-}C(R^1)O)]$ (R = Ph, R^1 = Ph **12a**, *n*Bu **12b**) and $Li_2[trans\text{-}Re_2(\mu\text{-}PPh_2)_2(CO)_6(ax\text{-}C(R)O)(ax\text{-}C(R^1)O)]$ (R = *n*Bu, R^1 = *n*Bu **13a**, Ph **13b**; R = Me, R^1 = Me **13c**, Ph **13d**) as precursor complexes. To 10 ml thf solution of $Re_2(\mu\text{-}PPh_2)_2(CO)_8$ **1** (150 mg, 0.155 mmol) one equiv RLi (R = Ph, Me, *n*Bu) in cyclohexane/ether solution was added at −90°C. After reaching room temperature a second equivalent LiR^1 (R^1 = Bu, Ph) was added. The formation of the lithium salts due to ^{31}P NMR and IR measurements was quantitative within 15 min. Subsequent removing of solvents in vacuo gave yellow lithium salts containing different amounts of thf.

cis-$Re_2(\mu\text{-}PPh_2)_2(CO)_6(ax\text{-}C(Ph)OEt)_2$ **14**. Within 30 min 30 ml CH_2Cl_2 solution of **12a** (0.155 mmol) and two equiv Et_3OBF_4 reacted at room temperature to **14**. The precipitate of $LiBF_4$ was filtered off, and the components of the solution were adsorbed on neutral Al_2O_3 as column material. The eluant CH_2Cl_2 separated only the product **14**, which gave orange crystals (yield 49%).

trans-$Re_2(\mu\text{-}PPh_2)_2(CO)_6(ax\text{-}C(R)OMe)$

(ax-$C(R^1)$OMe) (R = R^1 = *n*Bu **15a**, R^1 = Ph **15b**; R = Me, R^1 = Ph **15c**). As described for the *cis* dirhenium derivatives, each lithium salt **13b**–**c** reacts with two equiv Me_3OBF_4 in CH_2Cl_2 solution within 20 min at room temperature to the *trans* dicarbene. For product separation, the dicarbene and $LiBF_4$ were precipitated by addition of *n*-hexane (5 ml). Both products were filtered off and the dicarbene dissolved in CH_2Cl_2. The dicarbenes crystallized as yellow solids (yield 50–30%).

trans-$Mn_2(\mu\text{-}PPh_2)_2(CO)_6(ax\text{-}C(n\text{Bu})OEt)_2$ **16**. To **2** dissolved in thf one equiv BuLi in cyclohexane/ether solution was added at −50°C. After warming up to −10°C a second equiv BuLi was added. The solvents were removed in vacuo and the remaining Li salt reacted in CH_2Cl_2 solution with two equiv Et_3OBF_4 at 0°C. Product separation was done by TLC procedure yielding (33%) orange crystals.

Elementary analyses gave satisfactorily results.

3.3. Spectroscopic data

δ values ^{31}P NMR-spectra ($CDCl_3$, standard 85% H_3PO_4). Dimanganese monoacyl ions as **6ax** (thf) −29.9 (very broad, vb) (s, 2P, μ-P), **6eq** (thf) −22.4 (vb) (s, 2P, μ-P); **7ax** −27.5 (vb) (s, 2P, μ-P), **7eq** −23.4 (vb) (s, 2P, μ-P); **8ax** (CD_2Cl_2) −26.4 (vb) (s, 2P, μ-P), **8eq** −22.4 (vb) (s, 2P, μ-P). Dirhenium diacyl dianions as lithium salts, *cis* isomers (s, 2P, μ-P); **12a** (thf) −123.2 (s, 2P, μ-P), **12b** (thf) −122.9; *trans* isomers (s, 2P, μ-P) **13a** (thf) −116.3, −111.3 (CD_2Cl_2), **13b** (thf)

Table 2
Crystal data and refinement details

	5b	9ax	14	15b	16
Formula	$C_{37}H_{32}O_8P_2Re_2$	$C_{40}H_{30}O_8P_2Mn_2$	$C_{48}H_{40}O_8P_2Re_2^*CHCl_3$	$C_{44}H_{40}O_8P_2Re_2$	$C_{44}H_{48}O_8P_2Mn_2$
M_W	1038.9	810.4	1298.5	1131.1	876.6
Crystal system	Orthorhombic	Monoclinic	Monoclinic	Monoclinic	Monoclinic
Space group	$P2_12_12_1$	$P2_1/n$ (No. 14)	$P2/c$ (No. 13)	$P21/c$	$P21/n$ (No. 14)
a (Å)	9.624(2)	18.122(4)	21.685(4)	15.516(3)	9.391(3)
b (Å)	18.011(4)	11.745(2)	10.763(2)	16.707(3)	16.697(5)
c (Å)	21.391(4)	19.153(4)	21.771(4)	17.164(3)	13.708(4)
β (°)	116.75(2)	106.71(1)	107.27(3)	99.41(2)	
V (Å^3)	3708(1)	3640(1)	4867(2)	4249(2)	2120(1)
Z	4	4	4	4	2
D_c (g cm^{-3})	1.861	1.479	1.772	1.768	1.373
μ (mm^{-1})	6.659	0.835	5.252	5.819	0.722
θ range for data collection	2.2–26.1	2.1–27.6	2.1–27.6	2.4–27.6	2.4–27.6
Indep. data	4105	8408	11 255	6397	4894
Parameters	436	470	579	509	256
$R[F^2>2\sigma(F^2)]$	0.062	0.082	0.052	0.053	0.052
$wR[F^2]$	0.148	0.154	0.107	0.135	0.171
T(K)	293(2)	203(2)	293(2)	293(2)	203(2)

-114.6 -109.1 ($CDCl_3$), **13c** (thf) -116.5, **13d** (thf) -114.5. Dimanganese carbenes. **9ax** -36.9 (vb) (s, 1P, μ-P), **9eq** -39.6 (vb) (s, 1P, μ-P), -28.4 (vb) (s, 1P, μ-P). **10ax** -36.8 (vb) (s, 2P, μ-P), **10eq** -42.8 (vb) (1, 1P, μ-P) (partly coverd by the signal of the ax isomer), -25.3 (vb) (s, 1P, μ-P); **11ax** -36.6 (vb) (s, 2P, μ-P); **11eq** (small amount). Dimanganese dicarbene *trans*-$Mn_2(\mu\text{-}PPh_2)_2(CO)_6$(ax-C(*n*Bu)OEt)$_2$ **16** -34.8 (s, 2P, μ-P). Dirhenium dicarbenes, *cis* isomer **14** -129.8 (s, 2P, μ-P); *trans* isomers (s, 2P, μ-P) **15a** -126.5, **15b** -127.4, **15c** -127.7.

δ values ^{1}H NMR-spectra ($CDCl_3$, standard TMS). Dimanganese monoacyl ions **7ax** 2.5 (s (broad), 3H, CH_3), **7eq** 2.3 (s (broad) 3H, CH_3). Dimanganese carbenes, **9ax** 0.34 (t, 3H, CH_3, $^2J_{HH}=7.2$ Hz), 3.6 (q, 2H, OCH_2, $^3J_{HH}=7.2$ Hz), 6.86 (d, 2H, *o*-H (=(PPh), $^3J_{HH}=7.2$ Hz), 7.18–7.88 (m, 23H, Ph); **9eq** 1.63 (t, 3H, CH_3, $^3J_{HH}=7.1$ Hz), 3.99 (q, 2H, OCH_2) $^3J_{HH}=7.1$ Hz), 6.69 (d, 2H, *o*-H (=CPh), $^3J_{HH}=7.0$ Hz, 7.18–7.88 (m, 23H, Ph); **10ax** 0.4 (t, 3H, CH_3(OEt), $^3J_{HH}=7.2$ Hz), 3.08 (s, 3H, CH_3), 3.64 (q, 2H, OCH_2, $^3J_{HH}=7.2$ Hz), 7.17–7.80 (m, 20H, Ph); **10eq** 1.49 (t, 3H, CH_3(OEt), $^3J_{HH}=7.0$ Hz), 2.79 (s, 3H, Me), 4.33 (q, $^3J_{HH}=7.0$ Hz, 2H, OCH_2), 7.17–7.80 (m, 20H, Ph); **11ax** 0.4 (t, 3H, CH_3(OEt), $^3J_{HH}=7.1$ Hz), 0.96 (t, 3H, CH_3, $^3J_{HH}=6.7$ Hz) 3.37 (t, 2H, CH_2, $^3J_{HH}=7.8$ Hz), 3.6 (q, 2H, OCH_2, $^3J_{HH}=7.2$ Hz). Dirhenium carbenes. **4a** 0.26 (t, 3H, CH_3, $^3J_{HH}$), 3.44 (q, 2H, OCH_2), $^3J_{HH}=7.1$ Hz), 6.85 (d, 2H, *o*-H, (Ph), $^3J_{HH}=7.2$ Hz), 7.06–7.84 (m, 23H, Ph); **4b** 0.34 (t, 3H, CH_3, $^3J_{HH}=7.2$ Hz), 2.88 (s, 3H, CH_3), 3.51 (q, 2H, OCH_2, $^3J_{HH}=7.2$ Hz), 7.12–7.61 (m, 20H, Ph); **5a** 0.98 (t, 3H, CH_3, $^3J_{HH}=6.6$ Hz), 1.45–1.47 (m, 4H, CH_2), 3.12 (s, 3H, OCH_3), 3.23 (t, 2H, CH_2, $^3J_{HH}=7.5$ Hz), 7.11–7.60 (m, 20H, PPh); **5b** 1.36 (s, 9H, *t*Bu) 3.44 (s, 3H, OMe), 7.1–7.59 (m, 20H, Ph). *trans*-$Mn_2(\mu\text{-}PPh_2)_2(CO)_6$(ax-C(*n*Bu)OEt)$_2$ **16** 0.42 (t, 6H, CH_3, $^3J_{HH}=7.2$ Hz), 0.86 (t, 6H, CH_3, $^3J_{HH}=6.9$ Hz), 1.24 (m, 4H, CH_2), 1.34 (m, 4H, CH_2), 2.98 (t, 4H, CH_2, $^3J_{HH}=7.8$ Hz), 3.8 (q, 4H, OCH_2, $^3J_{HH}=7.2$ Hz), 7.05–7.7 (m, 20H, Ph). Dirhenium dicarbenes. **14** 0.72 (t, 6H, CH_3, $^3J_{HH}=7.2$ Hz), 3.8 (q, 8H, OCH_2, $^3J_{HH}=7.2$ Hz), 7.03–7.70 (m, 30H, Ph). **15a** 0.91 (t, 6H, CH_3, $^3J_{HH}=7.1$ Hz), 1.24 (m, 4H, CH_2), 1.35 (m, 4H, CH_2), 3.08 (t, 4H, CH_2, $^3J_{HH}=8.1$), 3.24 (s, 6H, OCH_3); 7.01–7.06 (m, 4H, *p*-H(Ph)), 7.15–7.20 (m, 8H, H(Ph)), 7.58–7.6 (s(broad), 8H, *o*-H(Ph)). **15b** 0.94 (t, 3H, CH_3, $^3J_{HH}=6.9$ Hz), 1.27–1.39 (m, 4H, $2CH_2$), 3.12 (s (broad), 5H, OCH_3 and CH_2), 3.17 (s, 3H, OCH_3), 6.41 (d, 2H, *o*-H(=C(PH)). **15c** 2.68 (s, 3H, CH_3), 3.10 (s, 3H, OCH_3), 3.14 (s, 3H, OCH_3, 6.41 (d, 2H, *o*-H(=CPh), $^3J_{HH}=8.2$ Hz).

IR data for υ(CO) absorption bands (cm^{-1}): Dimanganese acylmonoanions as lithium salts. **6ax**/**6eq** 2050 vs, 1998 m, 1980 s, 1959 m, 1928 s, 1911 vs, 1880 s, 1866 sh, 1556 w; **7ax**/**7eq** 2050 vs, 1996 s, 1957 m, 1926 s, 1903 vs, 1888 vs, 1874 sh, 1540 w; **8ax**/**8eq** 2050 vs, 1994 m, 1978 s, 1955 m, 1926 m, 1913 m, 1901 s, 1882 (broad) vs, 1861 sh, 1531 w. Dimanganese carbenes: **9ax** 2057 s, 2004 vs, 1982 m, 1973 sh, 1940 s, 1914 s; **9eq** 2057 vs, 2023 m, 2003 m, 1986 s, 1942 vs; **10ax** 2058 vs, 2004 vs, 1984 m, 1969 sh, 1934 s, 1907 vs; **10eq** 2052 vs, 2019 vs 1990 m, 1953 m, 1922 s, 1897 m; **11ax** 2058 s, 1999 vs, 1980 m, 1979 sh, 1936 s, 1905 s. 16 1982 s, 1920 vs, 1893 vs. Dirhenium dicarbenes: **14** 2025 vs, 2005 m, 1949 w, 1934 m, 1909 s; **15a** 1999 vs, 1924 s, 1893 vs; **15b** 2002 vs, 1928 s, 1901 vs, 1842 sh; **15c** 2004 vs, 1928 s, 1899 vs.

3.4. X-ray data collection, structure solution and refinement

Pertinent crystallographic data are summarized in Table 2. Intensities were collected on a Siemens R3m diffractometer using graphite monochromatized MoK_α radiation ($\lambda = 0.71073$ Å). Lp correction and empirical absorption correction via psi-scans were applied. Structures were solved by direct and conventional Fourier methods, full-matrix least-squares refinement on F^2; all but H-atoms refined anisotropically; H-atoms were refined at idealized positions with riding model. Program used for structure solution and refinement: SHELXTL V5 [26]. Lists of atomic coordinates, anisotropic displacement parameters, hydrogen atom coordinates and complete bond lengths and angles are available from the Fachinformationszentrum Karlsruhe, D-76344 Eggenstein-Leopoldshafen, on quoting the depository number CSD 407541 for **5b**, CSD 407542 for **9ax**, CSD 407543 for **14**, CSD 407544 for **15** and CSD 407545 for **16**.

References

[1] H.-J. Haupt, C. Heinekamp, U. Flörke, Inorg. Chem. 29 (1990) 2955.
[2] H.-J. Haupt, M. Schwefer, H. Egold, U. Flörke, Inorg. Chem. 36 (1997) 184.
[3] H.-J. Haupt, D. Petters, U. Flörke, J. Organomet. Chem., in press.
[4] (a) E.O. Fischer, A. Maasböl, Angew. Chem. 76 (1964) 645. (b) E.O. Fischer, Nato ASI Ser. C, 269 (1985) 1.
[5] T.C. Flood, J.M.O Connor, Comprehensive Organometallic Chemistry II, vol. 6, chapter 2, 9, 1995, pp. 22, 59, 196.
[6] (a) E.O. Fischer, E. Offhaus, Chem. Ber. 102 (1969) 2449. (b) E.O. Fischer, E. Offhaus, J. Müller, D. Noethe, Chem. Ber. 105 (1972) 3027. (c) E.W. Port, K.L. Walters, Inorg. Chim. Acta 26 (1978) 29. (d) R.J. McKinney, F.G.A. Stone, Inorg. Chim. Acta 44 (1980) L225.
[7] (a) C.P. Casey, C.R. Cyr, R.L. Anderson, D.F. Marten, J. Am. Chem. Soc. 97 (1975) 3053. (b) C.P. Casey, C.R. Cyr, J. Organomet. Chem. 57 (1973) C69.
[8] A.M. Garner, A. Irving, J.R. Flors, Organometallics 9 (1990) 2836.
[9] C. Alvarez-Toledano, A. Parlier, H. Rudler, M. Rudler, J.C. Daran, C. Knobler, Y. Jeannin, J. Organomet. Chem. 328 (1987) 357.
[10] J. Burnet, A. Capprucci, R. Chauvin, Organometallics 15 (1996) 5254.
[11] (a) W. Wang, J.A. Ramsden, A.M. Arif, J.A. Gadysz, J. Am. Chem. Soc. 115 (1993) 3824. (b) S.B. Fallom, W. Wang, A.M. Arif, J.A. Gadysz, Angew. Chem. 105 (1993) 937. (c) S.B. Fallom, W. Wang, A.M. Arif, J.A. Gadysz, Organometallics 16 (1997) 2008.
[12] T. Ye, M.A. Anthony, Compr. Org. Funct. Group Transform. 3 (1995) 507.
[13] S. Warwel, V. Liebermann, Makromol. Chem. Rapid Comm. 4 (1983) 423.
[14] M. Jung, R. Blum, Tetrahedron Lett. 43 (1977) 3791.
[15] U. Flörke, M. Woyciechowski, H.-J. Haupt, Acta Cryst. C44 (1988) 2101.
[16] E. Fritsch, T. Kerscher, K. Polborn, W. Beck, J. Organomet. Chem. 460 (1993) C25.
[17] D.H. Gibson, S.K. Mandal, K. Owens, J.F. Richardson, Organometallics 9 (1990) 1936.
[18] J.-A.M. Garner, A. Irving, J.R. Moss, Organometallics 9 (1990) 2836.
[19] C. Kelley, N. Lugan, M.R. Terry, G.L. Geoffroy, B.S. Haggerty, A.L. Rheingold, J. Am. Chem. Soc. 114 (1992) 6735.
[20] U. Schubert, Organometallics 1 (1982) 1085.
[21] H. Fischer, J. Schleu, G. Roth, Chem. Ber. 128 (1995) 373.
[22] U. Flörke, H.-J. Haupt, Acta Cryst. C50 (1994) 378.
[23] R.G. Hayter, J. Am. Chem. Soc. 86 (1964) 823.
[24] M. Woyciechowski, PhD thesis, Paderborn, 1989.
[25] E. Podell, A. Giraitis, J. Organomet. Chem. 22 (1957) 598.
[26] G.M. Sheldrick, SHELXTL V5. Siemens Analytical X-ray Instruments Inc., Madison, Wisconsin, USA, 1995.